Title

Carrier and Phonon Spectrum Modification in Quantum Dot Superlattices Designed for Thermoelectric Applications

Authors

Balandin, Alexander A.
Lazarenkova, Olga L.

Publication Date

2002-10-22

Fundamental Science of Energy 002

"CARRIER AND PHONON SPECTRUM MODIFICATION IN QUANTUM DOT SUPERLATTICES DESIGNED FOR THERMOELECTRIC APPLICATIONS"

Alexander Balandin and Olga L. Lazarenkova

October 2002

This paper is part of the University of California Energy Institute's (UCEI) Energy Policy and Economics Working Paper Series. UCEI is a multi-campus research unit of the University of California located on the Berkeley campus.

UC Energy Institute
2539 Channing Way, # 5180
Berkeley, California 94720-5180
www.ucei.org

Carrier and Phonon Spectrum Modification in Quantum Dot Superlattices Designed for Thermoelectric Applications

Alexander A. Balandin and Olga L. Lazarenkova
Department of Electrical Engineering
University of California – Riverside
Riverside, CA 92521 USA

E-mail: alexb@ee.ucr.edu

Abstract

Quantum dot superlattices have recently been proposed for thermoelectric applications. The predicted improvement of the thermoelectric figure of merit in such structures should come from the decreased lattice thermal conductivity due to additional boundary scattering and acoustic phonon spectrum modification, as well as change in the carrier transport and density of states. Here we outline a theoretical model to calculate carrier and phonon dispersion in such structures and present results for Ge/Si quantum dot superlattices. We argue that one can tune the mini-band carrier transport and phonon dispersion in such a way that electron-phonon coupling is suppressed. The latter may open up a novel way for the enhancement of the thermoelectric figure of merit.

1. Introduction

Quantum dot superlattices (QDS) e.g., multiple arrays of quantum dots, have recently been proposed for thermoelectric applications [1-3]. Initially it has been suggested that the predicted improvement in such structures should come from the decreased lattice thermal conductivity due to additional acoustic phonon scattering on quantum dots and "some sort of quantum confinement of carries" in quantum dots. At the same time, a simplistic mechanism of the process when carriers are confined inside the dots, and electrical conduction is due to carrier hopping (tunneling) between the dots does not lead to significant improvement in thermoelectric properties. Indeed hopping conductivity is characterized by low mobility values [4]. It is also unlikely that above-the-barrier transport due to thermal excitation or applied bias would significantly contribute to the current for the realistic conditions of device operation. The situations when the main current contribution comes from carrier transport through, for example, wetting layers fall to another category since in this case the structure is closer to conventional multiple quantum well structure. In order to achieve thermoelectric properties improvement not only via thermal conductivity decrease one has to envision some other mechanisms.

Thus, we argue that in order to achieve "electron transmitting – phonon blocking" regime, which is desirable for the thermoelectric material, it may be helpful to use *regimented* quantum dot arrays where carrier transport is facilitated by mini-band formation, while acoustic phonons are subject to additional resonant scattering. A proper selection of the parameters of such QDS may also allow for tuning of the electron – acoustic phonon interaction and its suppression to some degree.

In the following section we consider three-dimensionally (3D) regimented QDS with the strong coupling (wave function overlap) among the dots. QDS with 3D regimentation has already been reported in literature [5]. Strong coupling and regimentation leads to formation of 3D extended mini-bands instead of localized quantum dot states. This makes such structures analogous to artificial crystals, e.g. *quantum dot crystals* [6]. Such energy spectrum modification is expected to take place provided that the dot size is homogeneous and the dots are crystalline with low surface defect concentration. Formation of extended electron states and mini-bands have also already been observed in multiple quantum-dot arrays [4,7].

2. Theoretical Model

We calculate electron spectrum of QDS in the envelope wave function approximation applied to a potential barrier profile of choice. The one-electron Schrödinger equation for such a system is written as

$$\left[-\frac{\hbar^2}{2}\nabla_{\mathbf{r}}\frac{1}{m^*}\nabla_{\mathbf{r}}+V(\mathbf{r})\right]\varphi(\mathbf{r})=E\,\varphi(\mathbf{r}) \qquad (1)$$

where $\hbar$ is Plank's constant, $1/m^*$ is the reciprocal effective mass tensor, $\varphi(r)$ is the electron wave function, E is the electron energy, and the confining potential profile $V(\mathrm{r})$ corresponds to an infinite sequence of quantum dots of size L_x, L_y, and L_z separated by the barriers of thickness H_x, H_y, and H_z. The profile $V(\mathrm{r})$ is set to zero in the barrier region, while inside quantum dot it is equal to the band offset in the conduction (or valence) band of the considered material system taken with a negative sign. The information about band structure of the host materials is reflected in the reciprocal effective mass tensor $1/m^*$. The effect of strain was approximately taken into account by changing the value of the corresponding band offset. The confining potential $V(\mathrm{r})$ was considered to be a piece-wise uniform function.

Heat is carried by acoustic phonons. Acoustic phonon dispersion is strongly modified in QDS. In the long-wavelength limit, the dispersion can be described by a continuum model. For QDS made of semiconductors of cubic symmetry, such as Si and Ge with diamond lattice (O_h^7 space group), or A^3B^5 compounds with zincblende lattice (T_d^2 space group) the number of independent elastic stiffness constants in the elasticity equation reduces down to three:

$$\rho\frac{\partial^2 u_x}{\partial t^2}=\frac{\partial}{\partial x}c_{11}\frac{\partial u_x}{\partial x}+\frac{\partial}{\partial y}c_{44}\frac{\partial u_x}{\partial y}+\frac{\partial}{\partial z}c_{44}\frac{\partial u_x}{\partial z}$$
$$+\frac{\partial}{\partial x}c_{12}\frac{\partial u_y}{\partial y}+\frac{\partial}{\partial x}c_{12}\frac{\partial u_z}{\partial z}+\frac{\partial}{\partial y}c_{44}\frac{\partial u_y}{\partial x}+\frac{\partial}{\partial z}c_{44}\frac{\partial u_z}{\partial x}. \qquad (2)$$

Similar expressions for y- and z-components of the displacement vector **u** of a geometrical point inside the material of QDS with ($i = x,y,z$) coordinates can be obtained by cyclic exchange of (u_x, u_y, u_z) and (x, y, z). The elasticity Eqs. (2) in a non-uniform medium results from Euler-Lagrange equations for the system with cubical crystal lattice. The solution of these equations for QDS can be expressed in a plane wave form by analogy with regular bulk crystals

$$\mathbf{u}(\mathbf{r},t)=\mathbf{A}(\mathbf{r})\exp[i(\mathbf{q}\cdot\mathbf{r}-\omega t)]\ , \qquad (3)$$

where $|\mathrm{q}| = 2\pi/\lambda$ is the phonon wave vector, with phonon wavelength λ, r is coordinate vector, t is time, and ω is the phonon frequency. The eigenvalues of Eq. (2) in bulk material linearly depend on the phonon wave vector, as it should be in the continuum approximation.

We solve Eqs. (1-2) using the finite difference method (FDM). Details of the simulation procedure are reported elsewhere [8]. A simpler semi-analytical approach to calculate electron dispersion below the potential barrier in QDS with a model confining potential that allows for electron wave function separation has been reported in Ref. [6].

3. Results and Discussion

As an example material system we consider Ge quantum dots grown on (001) Si by the molecular beam epitaxy (MBE). Although state-of-the-art Ge/Si QDS are characterized only by partial regimentation, continuous progress in MBE self-assembly most likely will lead to synthesis of 3D regimented quantum dot superlattices similar to those reported in Ref. [5]. For simplicity we restrict our analysis to heavy-holes in Ge/Si QDS. This is done for two reasons. Firstly, most of the band-gap discontinuity between Si and Ge goes to the valence band. Secondly, the potential energy maximum in the valence band is located in Γ point, which greatly simplifies the model and justifies our omission of carrier Bloch functions from consideration.

Fig. 1 shows the heavy-hole dispersion in Ge/Si QDS calculated using FDM. The energy is given with respect to the position of the potential barrier. Double brackets for the wave vector notation are introduced to distinguish direction in quantum dot supra crystal from crystallographic directions.

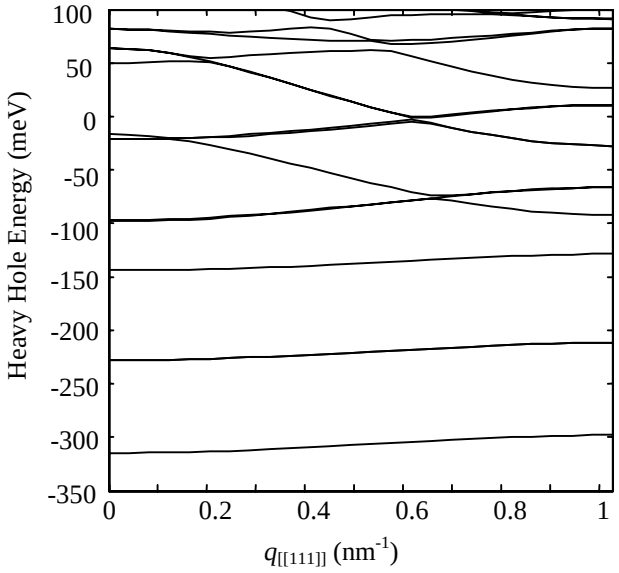

Figure 1. Heavy-hole dispersion in Ge/Si QDS with the following parameters: $L_x = L_y = 5$ nm, $L_z = 2.5$ nm, $H_x = H_y = 2.5$ nm, and $H_z = 1.25$ nm along [[111]] quasi-crystallographic direction. The depth of potential well is $V = 450$ meV. The energy in units of eV is counted from the position of the potential barrier.

One can see the transformation of discrete levels of isolated quantum dots to mini-bands in 3D regimented quantum dot arrays. Similar to bulk crystals, the energy in QDS has the full symmetry of the reciprocal lattice. In this artificial crystal some of the energy bands are degenerate in the center of the *quasi*-Brillouin zone (QBZ). Moving away from the point of high symmetry in the center of QBZ to a point of lower symmetry splits the energy branches. The width of mini-bands rapidly increases with shrinking of distance between quantum dots and may be up to dozens meV. The existence of the mini-bands means that electron (or hole) state are extended over the whole QDS structure instead of being confined in separate quantum dots. Their group velocity components strongly depend both on the mini-band number and the quasi-crystallographic direction. It is interesting to note that in an ideal artificial crystal, it is possible to achieve a very high electron velocity (on the same order of magnitude as the thermal velocity in the host material). This fact is explained by the small size of the quasi Brillouin zone in QDS as compared to the Brillouin zone in bulk crystals. It permits carriers to move easily under the influence of electric field. The latter leads to a much higher conductivity in a regimented quantum dot array compared to that of an array of randomly positioned quantum dots with the same size. Thus the power factor, which is proportional to electrical conductivity, increases leading to *ZT* improvement.

Fig. 2 shows electrical conductivity of a three-dimensional regimented *p*-doped Ge/Si QDS obtained on the basis of model developed in Ref. [6] under certain simplifying assumptions. In our calculations we took into account modification of heavy-hole energy spectrum only. The nonlinear behavior seen in Fig. 2 is explained by slope change of the carrier dispersion branches (changing of the effective sign of major carriers taking part in the conductivity) as quasi-Fermi level shifts up in energy.

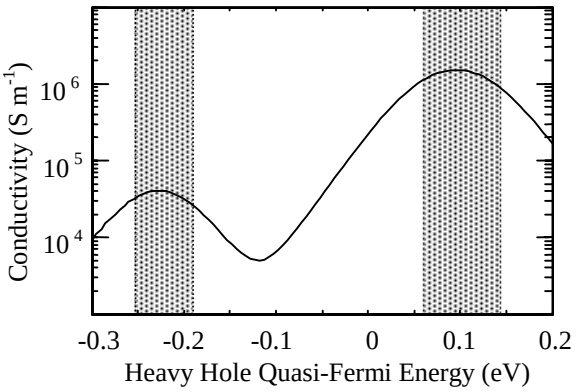

Figure 2. Electric conductivity at room temperature of simple cubical *p*-doped Ge/Si QDS with the following parameters: $L = 2.5$ nm, $H = 1.0$ nm, $V_e = 0.45$ eV, $m^*_W = 0.28\ m_0$, and $m^*_B = 0.49\ m_0$ at room temperature as a function of heavy hole quasi-Fermi energy. The depth of potential well is $V = 450$ meV. The energy in units of eV is counted from the position of the potential barrier. The constant relaxation time value is about 10^{-12} s. The gray stripes show the energy range of "almost free" motion of carriers over the whole QDS.

When quasi-Fermi level is lower then the lowest mini-band, only small part of the tail of Fermi distribution appears in the range of allowed energies. This situation is similar to ordinary conductivity of doped semiconductors and corresponds to quasi-semiconductor conductivity of QDS. When quasi-Fermy energy is inside a mini-band, carries in *kT* energy-range almost freely move inside the mini-band over the whole QDS. This corresponds to quasi-metallic conductivity of QDS, which is an order of magnitude larger then that in the quasi-semiconductor regime. The further shifting of the quasi-Fermi energy up to a mini-band gap leads to conductivity drop. This cycle repeats every time as E_F goes through a mini band. The presented result is valid for the low-field electrical conductivity, when the electronic mini-bands do not split into a Wannier-Stark ladder.

While regimentation of quantum dots makes it easy for carriers to move, phonons are effectively scattered by quantum dots interfaces. Solid lines in Fig. 3 present the phonon dispersion in [[111]] quasi-crystallographic direction calculated using FDM. There exist two different types of phonon modes in regimented QDS that emanated from bulk acoustic modes. These modes are quasi-acoustic ($\omega(\boldsymbol{q}=0)=0$) and quasi-optical ($\omega(q=0)\neq 0$).

Quasi-acoustic modes are nothing else but folded acoustic branches of the host material. The multiple reflection of phonons from periodical interfaces leads to a mini-gap formation at the Brillouin zone boundary. The degeneracy due to intersection of different branches is lifted everywhere except for the points of high symmetry. The value of the group velocity for the quasi-acoustic phonons in Ge/Si QDS lies between Si and Ge sound velocities and it is not defined by the volume fractions of two constituent materials. Even in solid alloys where atoms of two materials are randomly distributed elastic properties change almost linearly only in "one-mode behaved" systems such as $Na_{1-x}K_xCl$.

The compositional dependence of phonon energy in Si_xGe_{1-x} alloy is far from linear. In systems with a spatial regimentation like in 3D regimented QDS the deviation from linear dependence should increase.

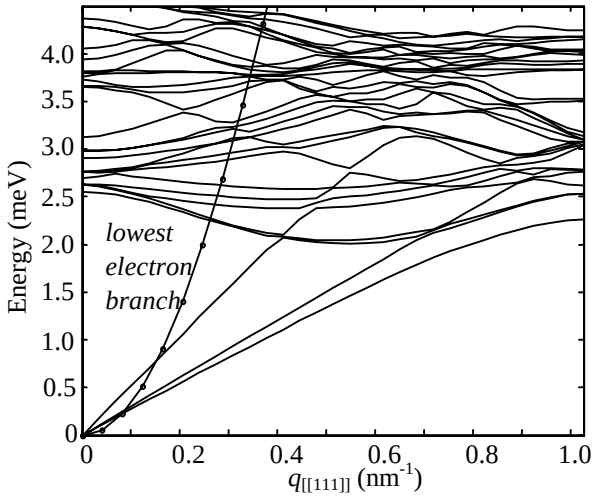

Figure 3. Phonon dispersion (solid lines) and the first heavy-hole mini-band (solid line with dots) shown along [[111]] quasi-crystallographic direction in Ge/Si QDS with the following parameters: $L_x = L_y = 5.0$ nm, $L_z = 2.5$ nm, $H_x = H_y = 2.5$ nm, and $H_z = 1.25$ nm. For convenience, the heavy-hole energy is counted from the mini-band minimum.

Quasi-optical modes correspond to "nearly standing" waves. One can view them as created by periodic scatters such as quantum dot interfaces. These modes can be induced inside quantum dots or in the space between them. A "true" standing wave would have a completely flat dispersion curve, which reflects the fact that this wave does not propagate through the crystal. In contrast, the dispersion branches of quasi-optical modes can have a minimum. The latter means that these modes propagate slowly going back and forth. We refer to these modes as quasi-optical since they have a nonzero energy in the center of the Brillouin zone, e.g. a cut-off frequency. At the same time one should emphasize that these modes also originate from acoustic bulk phonon modes. The regular optical phonon modes have much higher energy. In Ge/Si QDS of the considered geometry the lowest quasi-optical branch has the energy of about 2.6 meV at the zone center. In bulk Si the longitudinal optical (LO) and transverse optical (TO) phonon energies are $\hbar\omega_{LO}^{\Gamma} = \hbar\omega_{TO}^{\Gamma} =$ 64.3 meV. In bulk Ge they equal to $\hbar\omega_{LO}^{\Gamma} = \hbar\omega_{TO}^{\Gamma} =$ 37.2 meV. The emergence of many new quasi-optical phonon branches in QDS with low characteristic energy may dramatically modify carrier energy relaxation processes in such structures.

A possibility of suppression of carrier – acoustic phonon interaction or at least achieving its high anisotropy can be briefly explained as follows. Let us consider single-phonon-assisted processes, which are usually the most important ones. We compare heavy-hole and phonon dispersion branches along [[111]] quasi-crystallographic direction in Fig. 3. The first heavy-hole branch is shown in Fig. 3 with solid line marked with circles. A hole can scatter from its initial state $E(\mathbf{k}_i)$ to the final state $E(\mathbf{k}_f)$ with a phonon $\hbar\Omega(\mathbf{q})$ assistance if and only if both energy conservation $E(k_f) - E(k_i) = \hbar\Omega(\mathbf{q})$, and momentum conservation $\mathbf{k}_f - \mathbf{k}_i = \mathbf{q}$ laws are satisfied. Assuming linear acoustic phonon dispersion for small wave vectors, e.g. $\hbar\Omega(\mathbf{q}) = \mathbf{v}_g\mathbf{q}$, one can find from the above equations the condition for the allowed acoustic phonon-assisted transitions

.

$$\frac{E(k_f) - E(k_i)}{k_f - k_i} = \mathbf{v}_g \qquad (3)$$

Eq. (3) can be graphically interpreted as a horde to the hole dispersion with the slope equal to the acoustic phonon group velocity. In tetragonal ($d_x = d_y > d_z$) QDS the heavy-hole and phonon dispersion along [[100]] and along [[010]] quasi-crystallographic directions generally have the smallest value of the slope, while [[111]] (see Fig. 3) is the direction of the steepest branches. It is much larger than the phonon group velocity of any branch. It results in scattering suppression in approximately 80% of the Brillouin zone except for the small areas near the center and Brillouin zone boundary. Thus, the hole - single phonon scattering in QDS displays spatial anisotropy and suppression. The latter increases hole -phonon relaxation time, which is favorable for thermoelectric applications.

Moreover, inter-mini-band transitions with assistance of one phonon are forbidden for the considered structure. The mini-gap between the first two mini-bands shown in Fig. 1 $E_2 - E_1 \sim$ 80 meV - 100 meV is larger than the optical phonon energy. At the same time, multi-phonon scattering in QDS may play a significant role in energy relaxation processes due to the presence of many quasi-optical phonon branches (see Fig. 3). At room temperature, these low-energy branches should have a high population density in accordance with the Bose-Einstein statistics.

Flattening of phonon dispersion in regimented QDS may have additional positive effect on the thermoelectric figure of merit *ZT* related to the lattice thermal conductivity decrease. Initially, this mechanism has been proposed for in-plane phonon transport in free-surface or clamped-surface semiconductor quantum wells [9-10] and quantum wires [11]. It has been pointed out in Ref. [9-10] that acoustic phonon dispersion modification leads to a decrease of the in-plane phonon group velocity and corresponding increase of the phonon relaxation rates on impurities, defects, as well as in Umklapp processes. As a result, the phonon (lattice) thermal conductivity experiences significant drop along in-plane direction. The precondition for such desirable for thermoelectric applications modification of phonon dispersion is small width of the structure (much smaller than the phonon mean-free path) and significant difference in elastic constants between well (wire) material and the barrier [9-11]. As one can see from Fig. 3 a similar dispersion flattening in regimented QDS calculated for realistic elastic constant values may lead to the significant decrease in lattice thermal conductivity as well.

Conclusions

We obtained the carrier and phonon energy spectra in three-dimensional regimented quantum dot superlattices (QDS) proposed for thermoelectric applications. Coupling among quantum dots in such regimented structure results in formation of carrier mini-bands provided that the disorder in the system is small. The latter allows one to achieve high carrier mobility values in such structures. We also demonstrated that the acoustic phonon dispersion in QDS undergoes strong tunable modification, which may open up new possibilities of carrier – phonon scattering suppression and thermal conductivity decrease favorable for thermoelectric applications.

Acknowledgments

This work was supported in part by UC Energy Institute EST program and CRDF-MRDA project ME2-3010 on Low-Dimensional Thermoelectric Structures.

References

1. K.L. Wang and A.A. Balandin, *Quantum Dots: Physics and Applications*, in Optics of Nanostructured Materials (John Wiley & Sons, Inc., New York, 2001), edited by V. Markel and T. George, p. 515.
2. T.C. Harman, P.J. Taylor, D.L. Spears, and M.P. Walsh, *J. Electronic Materials*, **29** (1), L1 (2000).
3. A. Khitun, A. A. Balandin, J.L. Liu and K.L. Wang, *J. Appl. Phys*., **88**, 696 (2000).
4. H.Z. Song, K. Akahane, S. Lan, H.Z. Xu, Y. Okada, and M. Kawabe, *Phys. Rev. B*, **64**, 085303-1 (2001).

5. G. Springholz, M. Pinczolits, P. Mayer, V. Holy, G. Bauer, H.H. Kang, and L. Salamanca-Riba, *Phys. Rev. Lett*., **84**, 4669 (2000).
6. O.L. Lazarenkova and A.A. Balandin, *J. Appl. Phys*., **89**, 5509 (2001).
7. M.V. Artemyev, U. Woggon, H. Jaschinski, L.I. Gurinovich, and S.V. Gaponenko, *J. Phys. Chem*., **104**, 11617 (2000).
8. O.L. Lazarenkova and A.A. Balandin, *Phys. Rev. B* (in review, 2002).
9. A. Balandin and K.L. Wang, *Phys. Rev. B*, **58**, 1544 (1998).
10. A. Balandin and K.L. Wang, *J. Appl. Phys*., **84**, 6149 (1998).
11. J. Zou and A. Balandin, *J. Appl. Phys*., **89**, 2932 (2001).